PHYSICAL REVIEW VOLUME 163, NUMBER 3 15 NOVEMBER 1967

Mobility of Charge Carriers in Semiconducting Layer Structures

R. FIVAZ* AND E. MOOSER
Cyanamid European Research Institute, Cologny, Geneva, Switzerland
(Received 26 May 1967)

The electrical resistivities and the Hall constants of the compound semiconductors GaSe, MoS_2, $MoSe_2$, and WSe_2, which crystallize in layer structures, have been measured at temperatures ranging from 100 to 700°K. The Hall mobilities derived from these measurements are all of the order of 100 cm^2/V sec at room temperature, and they exhibit a temperature dependence of the form $\mu \propto (T/T_0)^{-n}$, where $n=2.1$ for GaSe, $n=2.6$ for MoS_2, and $n=2.4$ for $MoSe_2$ and WSe_2. A short-range interaction is discussed which couples the charge carriers in highly anisotropic layer structures to the nonpolar optical lattice modes. The relatively low room-temperature mobilities as well as the high values of the exponents n are explained in terms of the proposed interaction.

1. INTRODUCTION

IN order to detect possible nontrivial departures of the physical properties of layer structures from the properties of isotropic crystals, we have measured the temperature dependence of electrical resistivity and Hall coefficient of the semiconducting compounds GaSe, MoS_2, $MoSe_2$, and WSe_2, and from these measurements deduced the corresponding free-carrier mobilities. The structure of GaSe as well as the MoS_2 structure of the other three compounds consist of stacks of layers such that within each layer the atoms are held together by strong covalent forces, while the bonding between adjacent layers is of the weak van der Waals type. In Figs. 1(a) and 1(b) perspective views of individual layers of the GaSe and MoS_2 structures are reproduced.

In previous papers[1,2] we have discussed how pronounced structural anisotropies may affect the free-carrier motion in semiconductors. In particular, it was shown that in the structures considered here the free charge carriers tend to become localized within individual layers and thus to behave as if moving through a stack of independent layers. Moreover, it was found that this tendency is accompanied by a strong interaction between the free carriers and the optical phonons polarized normally to the layers. The mechanism of this interaction can readily be visualized by describing the layers as independent potential wells whose widths vary with the elastic deformations of the lattice. Within the adiabatic approximation the width of a layer determines the energy of localization of a free carrier in this layer. Variation of the width, therefore, represents a perturbation which gives rise to a friction of the carrier. Width-changing deformations occur in layers which like those of GaSe and MoS_2 are composed of several atomic planes, and they involve optical phonons polarized along the layer normal. In an external electric field the charge-carrier distribution may therefore be expected to relax predominantly through scattering by optical modes if the temperature is high enough for these modes to be excited.

2. EXPERIMENTAL PROCEDURE

Except for one sample (GaSe 11) which was pulled from the melt,[3] all the investigated crystals were produced by transport reaction. Reaction times and temperatures for the different batches of material, purity of the component elements, doping agents, and weight of the transport reagent per cubic centimeter of the reaction ampule are listed in Table I. Powders (Mo, W), pellets (Ga, Se) or chips (S) of the component elements

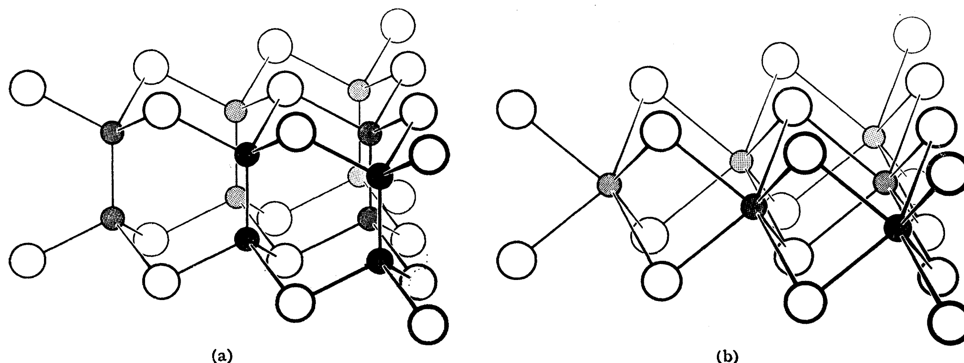

FIG. 1. The layers in (a) GaSe, (b) MoS_2, $MoSe_2$, WSe_2.

* Present address: Department of Physics, Iowa State University, Ames, Iowa.
[1] R. Fivaz and E. Mooser, Phys. Rev. 136A, 833 (1964).
[2] R. Fivaz, J. Phys. Chem. Solids 28, 839 (1967).
[3] A. Beck and E. Mooser, Helv. Phys. Acta 34, 370 (1961).

TABLE I. Doping, growth condition, conductivity type and room temperature resistivity of the samples.

Sample	Purity of components (%)		Added impurity (%)	Transport reagent	Growth time (h)	Temperatures of ampule ends (°C)	Conductivity type	Room-temperature resistivity (Ω cm)
GaSe								
11	Ga: 99.99%	Se: 99.999%	...	...	...	...	p	7.04×10^{3}
574/4 574/9			...	Iodine, 1.5 mg per cm^3 of ampule	168	800/760	p	8.8×10^{3} 6.8×10^{3}
580/1 580/4			...		624	870/840	n	7.0×10^{6} 2.00×10^{7}
581/1 581/3			10% Ge		296	870/840	n	5.16×10^{7} [a] 2.05×10^{7} [a]
582/1 582/2			...		600	870/840	n	1.32×10^{7} 1.67×10^{7}
586/1 586/2			10% Zn		296	870/840	p	5.52×10^{2} 1.10×10^{3}
588/2 588/4			5% Sn		288	870/840	n	1.25×10^{9} 1.8×10^{9}
600/1a			0.5% Zn		528	870/840	p	1.75×10^{3}
625/2	Ga: 99.9999%		...		504	870/840	n	9.1×10^{6}
635/2			10^{-1}% Zn		408	860/790	p	1.06×10^{2}
637/5 637/6			10^{-2}% Zn		264	850/760	p	25.2 39.4
638/5			10^{-3}% Zn		408	850/760	n	7.07×10^{6}
645/2			3×10^{-3}% Zn		168	850/760	p	1.12×10^{3}
MoS_2								
596a/1 596a/4 596a/5 596a/6	nonspecified (Wolframwerke Aarau)	S: 99.999%	...	Bromine, 5 mg/cm^3	160	1040/960	n	10.50 11.84 4.65 11.33
602/6 602/8			...		72	1035/985	n	3.38 8.14
608/1 608/2	Mo: 99.99%		...		264	1000/970	n	7.62 8.42
619/4			...		144	1030/980	n	4.95
$MoSe_2$								
597a/3 597a/5	Mo: nonspecified	Se: 99.999%	...	Bromine, 5 mg/cm^3	72	850/740	n	1.69 1.38
WSe_2								
601/1 601/3	W: nonspecified	Se: 99.999%	...	Bromine, 5 mg/cm^3	72	980/920	n	1.33 1.23

[a] At 100°C.

together with the doping agents in elemental form or as highly alloyed compounds were filled in appropriate amounts into quartz ampules. The ampules were then evacuated and the transport reagents (I, Br) added by sublimation. After sealing, the GaSe ampules were brought into the controlled gradient of a tube furnace in which the transport reaction took place in accordance with the data listed in Table I. The Mo and W samples, on the other hand, were allowed to react for up to 48 h at 700 to 1000°C prior to transport reaction, in order to reduce the danger of explosion. For the same reason, the ampules in which the Mo and W compounds were grown were smaller (20-cm long, 2-cm in diameter) than those used for GaSe (25-cm long, 4-cm in diameter).

The transport reaction products were monocrystalline flakes of more or less hexagonal shape. While the length of the flake edges always was of the order of 5 to 10 mm, the flake thickness varied from sample to sample between a few microns and several hundred microns. Microscopic inspection revealed no flaws other than slight irregularities of thickness resulting from the presence on the flake surfaces of growth spirals.[4] In order

[4] H. U. Boelsterli and E. Mooser, Helv. Phys. Acta 35, 538 (1962).

to avoid damage to the flakes during machining, they were cemented between two microscope slides and the resulting sandwiches cut with a diamond wheel. In this way samples of parallel-epipedic shape 2×7 mm^2 $\times$[flake thickness] were obtained which are adapted to measurements of resistivity and Hall voltage with the current flowing parallel to the layers and with the magnetic field applied perpendicular to them. Six contact arms protruded from the body of each sample. After removal of the protecting glass, these arms were gold coated by vacuum deposition and indium dots soldered to them. Finally spring loaded current and potential leads were pressed against the indium dots to establish the electrical connection between sample and apparatus. These contacts normally proved to be of sufficient quality to warrant accurate resistivity and Hall effect measurements. However, in some highly resistive samples the low-frequency noise generated by them was comparable to the Hall signal and it was necessary in these cases to take a whole series of measurements at the same temperature in order to obtain a representative average.

All measurements were carried out on zero-current bridges described earlier,[5] and every precaution was taken to eliminate spurious effects due to thermo-emf's and contact resistances. As discussed in Ref. 5, the accuracy of the measurements is not limited by the apparatus but by the contact noise and by the sample geometry. Because of the fragility of the samples the dimensions of the contact arms could not be made substantially smaller than those of the body of the sample itself, so that the geometrical factor of any one sample might be in error by as much as 100%. Since this error enters both resistivity and Hall constant as temperature-independent factor, it does not affect the slope of the logarithmically plotted Hall mobility curves corresponding to different samples of the same compound.

3. EXPERIMENTAL RESULTS

All measurements reported below were carried out with the current flowing perpendicular to the c axis of the crystals, i.e., in the plane of the layers and with the magnetic field applied parallel to this axis. Attempts to make four-probe measurements of resistivity with the current parallel to the c axis failed. Indeed, because of the small dimension of the samples along this axis the carrier injection at the contacts affects the bulk properties and gives rise to erratic results.

In all investigated samples the charge-carrier concentration n, as deduced from the Hall constant A according to

$$n=1/e|A|\,, \tag{1}$$

greatly exceeds the expected intrinsic concentration. It is safe, therefore, to assume that the majority carriers greatly outnumber the minority carriers and hence to calculate the Hall mobility μ from the corresponding resistivity ρ and Hall constant A according to

$$\mu=\text{const}\times|A|/\rho\,. \tag{2}$$

The mobility curves plotted in Figs. 4, 7, and 8 have been obtained in this way, putting the constant in Eq. (2) equal to unity. In addition to these curves, we also reproduce here the results of the Hall measurements (Figs. 2, 3, 5, and 6). The room-temperature values of the resistivities of the different samples are listed in Table I.

A. Gallium Selenide

In Fig. 2 the Hall constants of ten n-type samples of GaSe are plotted as functions of the inverse temperature and Fig. 3 contains similar plots for ten p-type samples. The impurity concentrations listed in the margin of the figures indicate the atomic percentages of impurities added to the reaction ampules before crystal growth. The effective impurity content of the doped samples is not known. Together with the data listed in Table I the Hall curves allow the following conclusions to be drawn:

1. At temperatures below 700°K the free-charge-carrier concentration in every sample is determined by impurities and/or crystalline imperfections. Attempts to attain intrinsic carrier concentrations above 700°K were discontinued because exposure of the samples to these temperatures leads to irreversible changes of their properties.

2. In agreement with results previously obtained

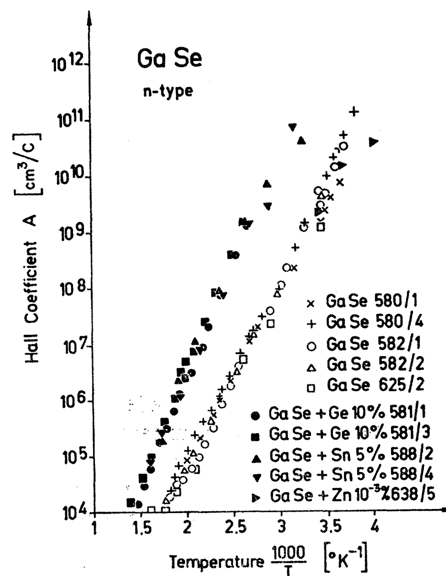

FIG. 2. Hall coefficient of n-type GaSe.

[5] R. Fivaz, Helv. Phys. Acta **36**, 1052 (1963).

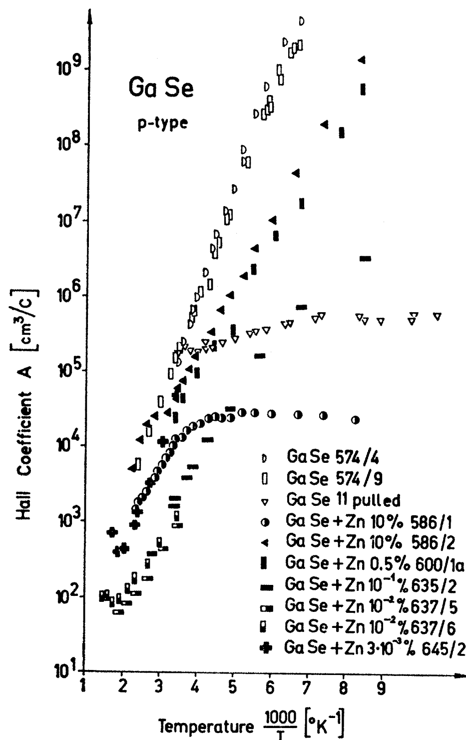

FIG. 3. Hall coefficient of p-type GaSe.

on melt-grown material[6,7] sample 11 which was pulled from the pure melt, shows p-type conduction.

3. Undoped, transport reacted samples are p-type, if the reaction time is less than about 200 h, and they are n type if the reaction time exceeds 400 h. The carrier compensation mechanism giving rise to this dependence of the conduction type on reaction time is not yet fully understood. It should be noted, however, that its exploitation represents the only means known at present with which to grow n-type GaSe.

4. Samples doped with a sufficient amount of Zn are p type regardless of reaction time. It is very likely, therefore, that Zn enters the GaSe lattice substitutionally on the cation sites, thus producing hydrogenlike acceptor centers. The activation energy ΔE of the Zn doped crystals as determined from the slope of the Hall curves lies between 0.16 and 0.18 eV, and thus differs markedly from that $\Delta E \approx 0.3$ eV found in undoped p-type samples.

5. Attempts to introduce donors into GaSe by adding Ge or Sn to the reaction ampule failed. Not only is the solubility of these elements in GaSe small—almost all the added Ge and Sn was unreacted after crystal growth—but the "doped" samples 581 and 588 have smaller charge-carrier concentrations than the pure n-type samples, and their activation energy $\Delta E \approx 0.85$ eV exceeds that $\Delta E \approx 0.65$ eV of the undoped material. These properties are suggestive of charge-carrier compensation and one can indeed imagine traces of Sn and/or Ge to produce complex impurity centers which will bring about such a compensation. However, in view of the growth time of 300 h, the compensation mechanism mentioned under 3 might well be responsible also for the properties of the samples 581 and 588.

In Fig. 4, the mobilities of electrons and holes in GaSe, computed from Hall effect and resistivity data according to Eq. (2), have been plotted as functions of the temperature.[8] The symbols used in Fig. 4 are the same as those in Figs. 2 and 3, so that corresponding Hall constants and mobilities can readily be recognized. As seen from the graph, electrons and holes behave similarly at temperatures above about 250°K: In a doubly logarithmic plot their mobilities μ_e and μ_h fall on straight lines of equal slope. The lines corresponding to the highest measured mobilities, are marked in the figure. Their analytical expressions are

$$\mu_e = 250(T/T_0)^{-2.1} \text{ cm}^2/\text{V sec}, \qquad (3a)$$

$$\mu_h = 50(T/T_0)^{-2.1} \text{ cm}^2/\text{V sec}, \qquad (3b)$$

where $T_0 = 300$°K. Keeping in mind the reservations made in Sec. 2 about the accuracy of the measurements,

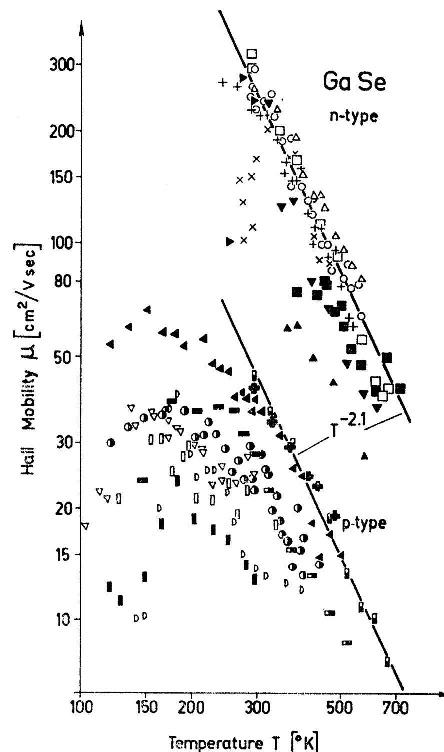

FIG. 4. Mobility of electrons and holes in GaSe.

[6] G. Fischer and J. L. Brebner, J. Phys. Chem. Solids **23**, 1363 (1962).

[7] G. Fischer, Helv. Phys. Acta **36**, 317 (1963).

[8] Some of the electron mobilities given here were erroneously ascribed to holes in Ref. 1.

we take (3a) and (3b) to represent the intrinsic mobilities of the charge carriers in GaSe.

B. Molybdenum and Tungsten Chalkogenides

In Figs. 5 and 6 the Hall constants of a series of single crystals of MoS_2, $MoSe_2$, and WSe_2 have been plotted as functions of the inverse temperature. From the slopes of these cruves—they correspond to activation energies lying between 0.07 and 0.16 eV—it follows that, although undoped, all samples have electron concentrations which are controlled by impurities. Their electron mobilities μ_e, however, are representative of intrinsic behavior above 200°K since, as seen from Figs. 7 and 8, they are very similar for different samples of the same material. The temperature dependences of μ_e derived from these graphs are

$$MoS_2: \quad \mu_e \cong 100(T/T_0)^{-2.6}\ \text{cm}^2/\text{V sec}, \quad (4)$$

$$MoSe_2, WSe_2: \quad \mu_e \cong 100(T/T_0)^{-2.4}\ \text{cm}^2/\text{V sec}, \quad (5)$$

where $T_0 = 300$°K.

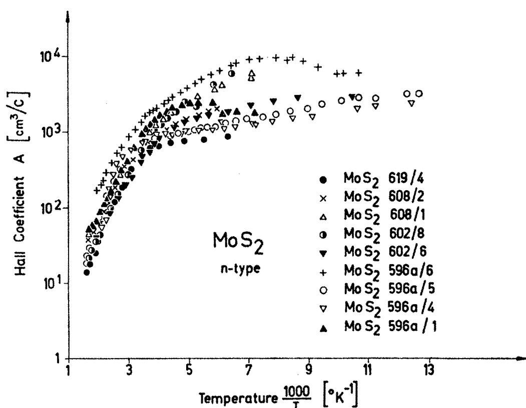

FIG. 5. Hall coefficient of n-type MoS_2.

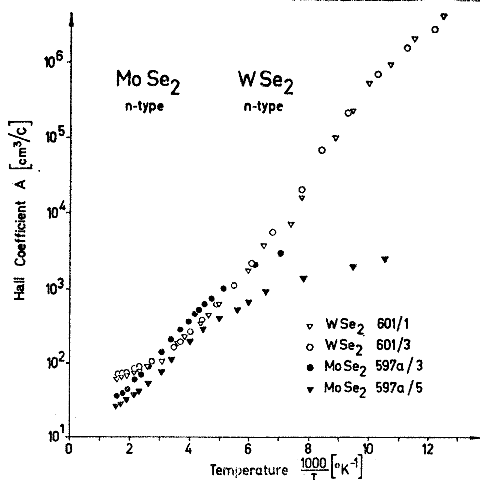

FIG. 6. Hall coefficient of n-type $MoSe_2$ and WSe_2.

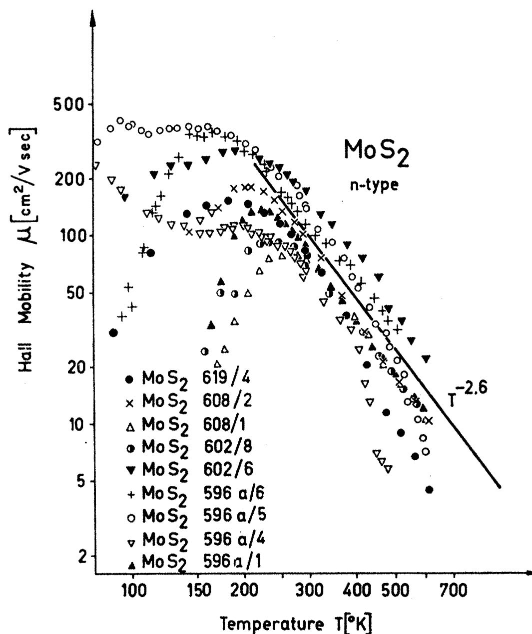

FIG. 7. Mobility of the electrons in MoS_2.

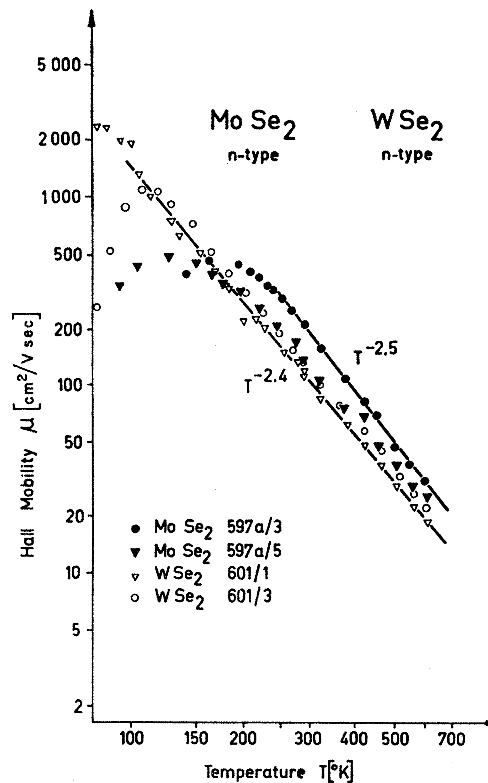

FIG. 8. Mobility of the electrons in $MoSe_2$ and WSe_2.

Attempts to dope MoS_2 with Nb resulted in p-type material. However, the corresponding hole mobilities $\mu_n \cong 10$ cm²/V sec are nearly temperature-independent and are therefore thought to be extrinsic.

Very few measurements of the transport properties have previously been made on these compounds. Hicks[9] reported a room-temperature mobility of the electrons in $MoSe_2$ of 15 cm^2/V sec and one of 100 cm^2/V sec of the holes in WSe_2. Both values were determined in pressed powder samples. Evans and Young[10] have measured the resistivity of natural MoS_2 crystals. Their room temperature value $\rho=13\ \Omega$ cm as well as the impurity activation energy $\Delta E=0.082$ eV derived from the resistivity versus temperature cruve agree well with the present results.

4. CALCULATION OF CHARGE-CARRIER MOBILITY

In order to determine the scattering mechanism responsible for the above experimental results we evaluate, in terms of conventional one-band transport theory, the mobility of charge carriers interacting with the modes of vibration of the perfect lattice. In these calculations, use is made of the results of the theory of layer structures as discussed in Ref. 2, to account for the large anisotropy of the physical parameters of layer structures.

A. Short-Range Interactions

The carrier-lattice interactions resulting from short-range forces give rise to finite carrier scattering probabilities for any vibrational mode of the lattice so that the equilibrium carrier distribution f_p in an external electric field can be described by the relaxation time formalism.[11] The drift mobility of carriers flowing along $\mathbf{i}$ in an electric field along $\mathbf{j}$ therefore is given by

$$\mu_{ij}=\sum_p e\tau_p \mathbf{v}_{pi}\mathbf{v}_{pj}\frac{\partial f_p{}^0}{\partial\epsilon_p}\,. \qquad (6)$$

where $\mathbf{v}_p$ is the group velocity of the Bloch state $\mathbf{p}$ of quasimomentum $\mathbf{p}$ and energy ϵ_p, where $f_p{}^0$ is the unperturbed carrier distribution and where the relaxation time τ_p is given by

$$\tau_p{}^{-1}=(\tau_p{}^+)^{-1}+(\tau_p{}^-)^{-1}\,, \qquad (7)$$

with

$$(\tau_p{}^\pm)^{-1}=\frac{2\pi}{\hbar}\sum_{p',k}|Q_{p,p',k}{}^\pm|^2\delta[\epsilon_{p'}-(\epsilon_p\pm\hbar\omega)]\,, \qquad (8)$$

and

$$Q_{p,p',k}{}^\pm=\langle n_k\pm1|\langle\mathbf{p}'|\sum_{ni}\sum_{n'i'}\boldsymbol{\eta}_{n'i'}\frac{\partial V_{ni}}{\partial\boldsymbol{\eta}_{n'i'}}|\mathbf{p}\rangle|n_k\rangle. \qquad (9)$$

Here $n_k=(e^{-\hbar\omega/kT}-1)^{-1}$ is the occupation number of the vibrational state $|n_k\rangle$ of wave vector $\mathbf{k}$; $\boldsymbol{\eta}_{ni}$ is the displacement of atom i in the cell positioned at $\mathbf{n}$, and V_{ni} is the potential field surrounding this atom and moving bodily with it (rigid-ion approximation). Introducing the cellular representation obtained by the Wannier transformation

$$|\mathbf{n}\rangle=\frac{1}{\sqrt{N}}\sum_p e^{i\mathbf{p}\mathbf{n}/\hbar}|\mathbf{p}\rangle\,,$$

where N is the number of cells per unit volume, we can neglect the small off-diagonal elements of the scattering matrix and thus have

$$Q_{\mathbf{p},\mathbf{p}',k}{}^\pm=(n_k{}^\pm)^{1/2}\sum_{ni}\sum_{n'i'}\langle\mathbf{n}|\boldsymbol{\eta}_{n'i'}\frac{\partial V_{ni}}{\partial\boldsymbol{\eta}_{n'i'}}|\mathbf{n}\rangle e^{i(\mathbf{p}-\mathbf{p}')\mathbf{n}/\hbar}\times\delta(\mathbf{p}',\mathbf{p}\pm\hbar\mathbf{k})\,, \qquad (10)$$

where $n_k{}^+=n_k$, $n_k{}^-=n_k+1$.

Evaluation of (10) requires knowledge of the electronic states. As shown in Ref. 2 the spectrum of the free carriers in layer structures can be written as the sum of an effective-mass term and a tight-binding term:

$$\epsilon(\mathbf{p})=\frac{p_x{}^2+p_y{}^2}{2m_x}+2I_z\left(\cos\frac{p_zd_z}{\hbar}-1\right)\,, \qquad (11)$$

where m_x is the effective resistance to an acceleration of the carriers along the plane of the layers, d_z the interlayer spacing and where I_z is the small overlap energy associated with the weak van der Waals bonding between adjacent layers. Since in the x, y plane the effective-mass approximation holds, the interference factor in (10) can be evaluated by a continuous approximation. Defining a Wigner-Seitz disk of radius ρ and area Σ we find

$$\sum_n e^{i(\mathbf{p}-\mathbf{p}')\mathbf{n}/\hbar}=\sum_{n_x}e^{i(\mathbf{p}_x-\mathbf{p}_x')\mathbf{n}_x/\hbar}=\frac{1}{\Sigma}\int_\Sigma e^{i(\mathbf{p}_x-\mathbf{p}_x')\mathbf{x}/\hbar}d\mathbf{x}$$
$$=\frac{J_1(t)}{t/2}=1-t^2/8+\cdots\,,$$
$$t=|\mathbf{p}_x-\mathbf{p}_x'|\rho/\hbar\,,$$

where J_1 is the Bessel function of the first kind, $\mathbf{x}$ the radius vector in the x,y plane and where the index x refers to quantities defined in this plane. As in the corresponding three dimensional situation, the interference factor is thus found to be close to unity for the small values of $|\mathbf{p}_x'-\mathbf{p}_x|$ compatible with a weakly degenerate carrier gas.

Except for a small range near the origin, the density of states $D(\epsilon)$ derived from the spectrum (11) is constant

$$D(\epsilon)=(m_xN_z/2\pi^2\hbar^2)\cos^{-1}(1-\epsilon/2I_z)\,,\quad \text{for}\quad 0\leqq\epsilon\leqq4I_z\,, \qquad (12)$$
$$=(m_xN_z/2\pi\hbar^2)=D_2\,,\quad\text{for}\quad \epsilon\geqq4I_z\,,$$

where N_z is the number of layers per unit length along the z axis. The derivative of this density of states is non-

[9] W. T. Hicks, J. Electrochem. Soc. **111**, 1058 (1964).

[10] B. L. Evans and P. A. Young, Proc. Roy. Soc. (London) **A284**, 402 (1965).

[11] See e.g.: A. C. Beer, *Galvanomagnetic Effects in Semiconductors* (Academic Press Inc., New York, 1963), Chap. 25.

zero only in the interval $0 \leqq \epsilon \leqq 4I_z$ at the boundaries of which it is infinite. In calculating integrals of the form

$$A = \int_0^\epsilon f(\epsilon')D(\epsilon')d\epsilon' = F(\epsilon')D(\epsilon')\Big|_0^\epsilon - \int_0^\epsilon \frac{dD(\epsilon')}{d\epsilon'} F(\epsilon')d\epsilon',$$

where

$$F(\epsilon) = \int_0^\epsilon f(\epsilon')d\epsilon'$$

we can, therefore, approximate $dD/d\epsilon$ by the sum of two properly normalized δ functions and obtain

$$A \cong F(\epsilon)D_2 - \int_0^\epsilon F(\epsilon')\frac{D_2}{2}[\delta(\epsilon') + \delta(\epsilon' - 4I_z)]d\epsilon' \cong D_2[F(\epsilon) - \tfrac{1}{2}F(4I_z)]. \tag{13a}$$

For small I_z this can be further simplified to

$$A \cong D_2 F(\epsilon) . \tag{13b}$$

With the above approximations the carrier mobility is now readily evaluated in terms of a relaxation time of the form $\tau = \tau_0 \epsilon^\alpha$. Indeed, it follows from (11) and (13a) that the "horizontal" mobility μ_{xx} of carriers moving in the plane of layers is

$$\mu_{xx} = \frac{e\tau_0}{m_x}(kT)^\alpha \alpha! \frac{1 - (\alpha+1, 2I_z/kT)!/(\alpha+1)!}{1 - (1, 2I_z/kT)!}, \tag{14}$$

where $(a,b)!$ is the incomplete factorial[12] tending towards zero like $b^{a+1}/a+1$ as b goes to zero. Within the approximation (13a) the mobility μ_{xx}, therefore is independent of I_z/kT for an energy-independent relaxation time ($\alpha = 0$).

By inserting the group velocity derived from (11)

$$v_z = \frac{\partial \epsilon}{\partial p_z} = -\frac{2I_z d_z}{\hbar} \sin \frac{p_z d_z}{\hbar}$$

into Eq. (6), we obtain the "vertical" mobility μ_{zz} of carriers moving perpendicularly to the layers in terms of μ_{xx}:

$$\mu_{zz} = \mu_{xx} \frac{m_x d_z^2}{\pi \hbar^2} \frac{I_z^2}{kT} . \tag{15}$$

We thus have the result that the ratio μ_{xx}/μ_{zz}, which measures the anisotropy of conductivity, is proportional to the inverse square of the overlap energy I_z and becomes very large for weak interaction between adjacent layers. Finally we add that with (13a) the ratio

$$\frac{\mu_{xx}^{\text{Hall}}}{\mu_{xx}^{\text{drift}}} = \frac{(1/m_x) \sum_p \tau_p^2 v_x v_x (\partial f_p^0/\partial \epsilon_p)}{(\sum_p \tau_p v_x v_x (\partial f_p^0/\partial \epsilon_p))^2}$$

of the horizontal Hall and drift mobilities is found to be:

$$\frac{\mu_{xx}^{\text{Hall}}}{\mu_{xx}^{\text{drift}}} = \frac{2\alpha+1}{[(\alpha+1)!]^2}, \tag{16}$$

which, for an energy-independent relaxation time, is equal to unity.

Turning our attention now to the calculation of the relaxation time we note that only phonons with small wave vectors can scatter the particles of a weakly degenerate gas. We therefore need to evaluate the scattering matrix (10) only in the limit $\mathbf{k} = 0$. In this limit acoustic phonons represent bodily motions of cells with respect to one another ($\boldsymbol{\eta}_{ni} = \boldsymbol{\eta}_{ni'}$), while optical phonons describe internal distortions of undisplaced cells ($\boldsymbol{\eta}_{ni} = \boldsymbol{\eta}_{n'i}$). Moreover, applying the identity

$$\sum_k \boldsymbol{\eta}_k \frac{\partial \bar{V}_i}{\partial \boldsymbol{\eta}_k} = \sum_{k<l} \sum (\boldsymbol{\eta}_k - \boldsymbol{\eta}_l) \frac{\partial \bar{V}_i}{\partial(\boldsymbol{\eta}_k - \boldsymbol{\eta}_l)},$$

with $\bar{V}_i = \langle \mathbf{n} | V_{ni} | \mathbf{n} \rangle$ and neglecting small three-center terms with $i \neq k \neq l$ we obtain after some rearrangement:

$$\sum_i \sum_{n'i'} \boldsymbol{\eta}_{n'i'} \frac{\partial \bar{V}_{ni}}{\partial \boldsymbol{\eta}_{n'i'}} = \sum_i \sum_{n' \neq n} (\boldsymbol{\eta}_{ni} - \boldsymbol{\eta}_{n'i}) \sum_{i'} \frac{\partial \bar{V}_{ni}}{\partial(\boldsymbol{\eta}_{ni} - \boldsymbol{\eta}_{n'i'})} \tag{17a}$$

for the acoustic modes, and

$$\sum_i \sum_{n'i'} \boldsymbol{\eta}_{n'i'} \frac{\partial \bar{V}_{ni}}{\partial \boldsymbol{\eta}_{n'i'}} = \sum_i \sum_{i' \neq i} (\boldsymbol{\eta}_{ni} - \boldsymbol{\eta}_{ni'}) \sum_{n'} \frac{\partial \bar{V}_{ni}}{\partial(\boldsymbol{\eta}_{ni} - \boldsymbol{\eta}_{n'i'})} \tag{17b}$$

for the optical modes.

Equation (17a) can be evaluated in the continuous approximation which describes the atomic motion in terms of local dilatations of the lattice. In layer structures only the horizontal dilations significantly modify the potential, the influence of the vertical ones being negligible because of the weakness of the van der Waals forces between layers. Thus, the carriers only interact with the horizontally polarized acoustic modes. By standard procedures[13] the corresponding energy-independent relaxation time is found to be

$$\tau^{-1} = (2m_x/\hbar^3)(\epsilon_x^2/N_x M_c s_x^2)kT , \tag{18}$$

[12] See e.g.: E. Jahnke and F. Emde, *Tables of Functions* (Dover Publications Inc., New York, 1945).

[13] See e.g.: J. M. Ziman, *Electrons and Phonons* (Clarendon Press, Oxford, England, 1960), Chap. 10.

where ϵ_x is the relevant deformation potential, N_x the number of cells per unit layer area, M_c the mass of a cell, and s_x the sound velocity in the layer. Acoustic-mode scattering therefore leads to a charge-carrier mobility which is inversely proportional to T:

$$\mu_{xx}=\frac{e}{2\hbar}\left(\frac{\hbar^2}{m_x}\right)^2\frac{N_xM_cs_x^2}{\epsilon_x^2}\frac{1}{kT}. \tag{19}$$

This unfamiliar temperature dependence—in isotropic media $\mu\sim T^{-3/2}$—is the result of the special form (12) of the density of states in layer structures.

In the optical case, the sum of the polarization vectors over a cell is known to vanish for small **k**. Moreover, if the atoms have a nearly spherically symmetric environment, the gradients $\partial\bar{V}/\partial\eta$ depend little on direction, and the sum (17b) is very small. Optical scattering can therefore be neglected in most quasi-isotropic (nonpolar) crystals. The large anisotropy in layer structures, however, gives rise to strongly direction-dependent gradients $\partial\bar{V}/\partial\eta$ and thereby leads to a coupling of the carriers to those optical modes which correspond to fluctuations of the layer thickness. In order to show this we first of all note that each layer of the considered crystals has a horizontal mirror plane. Thickness-modulating modes therefore correspond to the relative vertical motion of identical atoms each of which is the mirror image of the other. Since the center of mass of each atom and its mirror image is unaffected by this motion, no first-order dipoles are produced although not all atoms of the layer necessarily carry the same effective charge. The present modes therefore are "homopolar" as distinct from "polar" modes which give rise to first-order dipoles. The coupling of the carriers to polar modes will be considered later.

In vertically polarized homopolar modes, an atom and its mirror image vibrate in counterphase, and since the gradients $\partial\bar{V}/\partial\eta_z$ along the z direction are large and have different signs on opposite sides of the mirror plane, one finds

$$\sum_{ni}\sum_{n'i'}\eta_{n'i'}\frac{\partial\bar{V}_{ni}}{\partial\eta_{n'i'}}=\left(\frac{\hbar}{2MN\omega}\right)^{1/2}\frac{\epsilon_z}{a}, \tag{20}$$

where

$$\epsilon_z/a\sqrt{M}=\sum_{jj'}\frac{2}{\sqrt{M_{j'}{}^0}}\langle\mathbf{n}|\frac{\partial V_j}{\partial\eta_{j'z}{}^0}|\mathbf{n}\rangle.$$

N is the number of cells per unit volume, j enumerates the pairs {atom, mirror image}, and the index 0 refers to one of the partners of a pair. $M_j{}^0$ is the effective mass of this partner and depends on the detailed arrangement of masses and forces in the unit cell. By (20) a cellular oscillator of reduced mass M, linear equilibrium dimension a, and frequency ω is defined, whose vibrations affect the carrier energy through the deformation potential ϵ_z. This definition established the connection between the present atomic description of layer structures and the qualitative one mentioned in the Introduction, in which each layer corresponds to a potential well of variable width.

Introducing a coupling constant

$$g^2=(m_x/4\pi MN_x)(\epsilon_z/a\hbar\omega)^2, \tag{21}$$

which measures the number of virtual quanta coupled to a carrier, and making use of the results (A10) and (A11) evaluated in the Appendix, we obtain

$$(\tau^+)^{-1}=4\pi\omega g^2(e^{\hbar\omega/kT}-1)^{-1} \tag{22}$$

$$\begin{aligned}(\tau^-)^{-1}&=4\pi\omega g^2e^{-\hbar\omega/kT} && \text{for } \epsilon\geqq\hbar\omega\\ &=0 && \text{for } \epsilon<\hbar\omega.\end{aligned} \tag{23}$$

With (22) the horizontal mobility $\mu_{xx}{}^+$ corresponding to carrier scattering by phonon absorption is found to be

$$\begin{aligned}\mu_{xx}{}^+&=\frac{e}{4\pi m_x\omega g^2}(e^{\hbar\omega/kT}-1)\\ &=\frac{9}{g^2\hbar\omega}\frac{m}{m_x}(e^{\hbar\omega/kT}-1)\ \text{cm}^2/\text{V sec},\end{aligned} \tag{24}$$

where m is the electron mass and where $\hbar\omega$ is measured in units of 10^{-2} eV. Finally, taking into account (23), the mobility for scattering involving emission as well as absorption of phonons can be expressed in terms of $\mu_{xx}{}^+$:

$$\mu_{xx}=\mu_{xx}{}^+\left\{1-\frac{1-e^{-\hbar\omega/kT}}{2-e^{-\hbar\omega/kT}}[1-(1,\ \hbar\omega/kT)!]\right\}. \tag{25}$$

The function in brackets varies slowly between 1 and its minimum value ~0.7 which occurs at $\hbar\omega\cong kT$. In comparing theory and experiment we will, therefore, always assume μ_{xx} to be given by Eq. (24).

According to (20) the coupling of the free carriers to the optical modes is proportional to the vertical gradient of the potential. On the average this gradient is considerably larger than the horizontal one which, in accordance with (18), gives rise to the coupling with the acoustic modes. At sufficiently high temperatures *optical scattering, therefore, dominates in layer structures*, a fact which is reflected in a strong dependence of the carrier mobility on temperature. From (24) one does indeed find that around $T=T_0$:

$$\mu=\mu_0(T/T_0)^{-n}, \tag{26}$$

where

$$n=\frac{(\hbar\omega/kT_0)e^{\hbar\omega/kT_0}}{e^{\hbar\omega/kT_0}-1}>1.$$

This result, obtained by a perturbation calculation, applies only to carriers which interact weakly with the lattice. If the coupling constant g^2 exceeds a critical value, which within the tight-binding approximation was shown[1] to be $g_{\text{crit}}{}^2=\frac{1}{2}$, the carrier-lattice interaction is strong and each carrier is selftrapped in a

volume of the order of the unit cell. Thus a lower limit

$$\mu_{xx} \geq 18 \frac{m}{m_x} \frac{e^{\hbar\omega/kT}-1}{\hbar\omega} \text{ cm}^2/\text{V sec} \tag{27}$$

for the mobility of free carriers in layer structures is established. By analogy to the case of the strongly coupled "small" polaron[14] it is expected that for $g^2 > g_{\text{crit}}^2$ the mobility drops to much smaller values and increases exponentially with temperature. However, no detailed theory has as yet been developed for the transport of charge carriers which are selftrapped by short-range forces in a semiconductor of large bandwidth.[15]

B. Long-Range Interactions

In a crystal whose atoms carry effective charges the lattice vibrations give rise to polarization waves to which the carriers couple via the long-range Coulomb forces. For an isotropic medium with low- and high-frequency dielectric constants ϵ_0 and ϵ_∞, respectively, this "polaron" interaction has matrix elements of the form[13]:

$$Q_{\mathbf{p},\mathbf{p}',\mathbf{k}}^{\pm} = i(4\pi)^{1/2} e^2 \hbar\omega \left(\frac{1}{\epsilon_\infty} - \frac{1}{\epsilon_0}\right) \frac{1}{k} \times \delta(\mathbf{p}', \mathbf{p} \pm \hbar\mathbf{k}) (n_k^{\pm})^{1/2}. \tag{28}$$

In layer structures ω, ϵ_0, and ϵ_∞ are anisotropic. Thus, from an analysis of their infrared measurements on GaSe, Leung *et al.*[16] find $(\epsilon_{0x}/\epsilon_{0z}) = 1.36$ and $(\epsilon_{\infty x}/\epsilon_{\infty z}) = 1.18$, in good agreement with the value $(\epsilon_x/\epsilon_z) = 1.26$ derived from the birefringence measurements of Brebner and Déverin[17] on the same material at $\lambda = 7000$ Å. Obviously these anisotropies are small compared to the very large one of the carrier overlap energy on which the present model is based. In evaluating the mobility resulting from polar scattering we will, therefore, neglect them. Introducing an effective Fröhlich coupling constant[18]

$$\gamma = e^2 (m_x/2\hbar^3\omega)^{1/2} \left(\frac{1}{\epsilon_\infty} - \frac{1}{\epsilon_0}\right), \tag{29}$$

which can be treated as a phenomenological quantity, we obtain, for transitions involving absorption of a polar phonon

$$|Q_{\mathbf{p},\mathbf{p}',\mathbf{k}}|^2 = \frac{4\pi\gamma}{k^2} \left(\frac{2\hbar}{m_x\omega}\right)^{1/2} (\hbar\omega)^2 n_k \delta(\mathbf{p}', \mathbf{p} + \hbar\mathbf{k}). \tag{30}$$

Since this matrix element is infinite for $\mathbf{k} = 0$, the relaxation time formalism breaks down, and the transition probability must be evaluated by the variational method,[13] maximizing the entropy produced by the scattering. In this treatment the equilibrium carrier distribution f_p^0 is assumed to be perturbed by the amount

$$f_p - f_p^0 = -\Phi_p \frac{\partial f_p^0}{\partial \epsilon_p}, \tag{31}$$

where

$$\Phi_p = \sum_l \Phi_l(\epsilon_p)^l \mathbf{p} \cdot \mathbf{u}/\hbar.$$

$\mathbf{u}$ is the unit vector along the electric field and the Φ_l are the variational parameters. In the zero-order approximation we put $\Phi_l = 0$ for $l \neq 0$. The carrier density n, the current density $\mathbf{j}$ and the rate $\dot{S}$ of entropy production are then defined by

$$n = \sum_p f_p^0,$$

$$\mathbf{j} = -\sum_p e\mathbf{v}_p \Phi_p \frac{\partial f_p^0}{\partial \epsilon_p},$$

$$\dot{S} = \sum_{p,p',k} \frac{2\pi}{\hbar} \frac{(\Phi_p - \Phi_{p'})^2}{2T} |Q_{p,p',k}|^2 \times \delta(\epsilon_{p'} - \epsilon_p + \hbar\omega) f_p^0 (1 - f_p^0), \tag{32}$$

and the mobility is given by

$$\mu = j^2/enT\dot{S}. \tag{33}$$

With the electric field in the x,y plane i.e., parallel to the layers, conservation of momentum results in

$$(\Phi_p - \Phi_{p'})^2 = (\mathbf{k}_x \cdot \mathbf{u}_x)^2 = \tfrac{1}{2} k_x^2, \tag{34}$$

where the factor $\frac{1}{2}$ is the mean square of the cosine of all possible angles between $\mathbf{k}_x$ and the direction $\mathbf{u}_x$ of the field. With (34)

$$\dot{S} = \frac{2\pi^2\gamma}{kT} \left(\frac{2\hbar}{m_x\omega}\right)^{1/2} (\hbar\omega)^2 n_k \sum_{p,k} \frac{k_x^2}{k_x^2 + k_z^2} \times \delta(\epsilon_{p+\hbar k} - \epsilon_p + \hbar\omega) f_p^0 (1 - f_p^0)$$

and after summing over $\mathbf{k}$ in the way indicated in the Appendix [see formula (A14)]:

$$\dot{S} \cong \frac{2\pi\gamma}{kT} \frac{m_x}{\hbar^2} (\hbar\omega)^2 n_k \sum_p f_p^0 (1 - f_p^0) \left[1 + \left(\frac{\epsilon_p}{\hbar\omega}\right)^{1/2}\right].$$

Within the approximations (13a) the summations over $\mathbf{p}$ are then straightforward and one finds the mobility μ_{xx} along the field:

$$\mu_{xx} = \frac{e}{m_x\omega} \frac{1}{2\pi\gamma} \frac{kT/\hbar\omega}{1 + (\frac{1}{2})!(kT/\hbar\omega)^{1/2}} (e^{\hbar\omega/kT} - 1). \tag{35}$$

By its derivation (35) is valid for drift mobilities only. As can be seen from an extension of the variational

---

[14] E. L. Nagaev, Fiz. Trevd. Tela 4, 2201 (1962) [English transl.: Soviet Phys.—Solid State 4, 1611 (1963)].
[15] Y. Toyozawa, *Polarons and Excitons* (Oliver and Boyd, London, 1962).
[16] P. C. Leung, G. Andermann, W. G. Spitzer, and C. A. Mead, J. Phys. Chem. Solids **27**, 849 (1966).
[17] J. L. Brebner and J.-A. Déverin, Helv. Phys. Acta **38**, 650 (1965).
[18] G. R. Allcock, Advan. Phys. **5**, 412 (1956).

method,[13] the same result does, however, also hold for Hall mobilities.

In the neighborhood of T_0, we can again express the temperature dependence of μ as

$$\mu=\mu_0(T/T_0)^{-n}$$

where, in accordance with (35):

$$n=\frac{(\hbar\omega/kT_0)e^{\hbar\omega/kT_0}}{e^{\hbar\omega/kT_0}-1}-1+\frac{(\frac{1}{2})!}{2}\frac{(kT_0/\hbar\omega)^{1/2}}{1+(\frac{1}{2})!(kT_0/\hbar\omega)^{1/2}}. \quad (36)$$

At high enough temperatures $kT_0\gtrsim\hbar\omega$ the last term in (36) is negligibly small. Denoting the exponent (36) by n_{pol} and that (26) by n_{hom}, we therefore have

$$n_{\text{pol}}\cong n_{\text{hom}}-1$$

and we see that if the carrier mobility is limited by polar scattering, then its variation with temperature is smaller than if it is limited by the "homopolar" scattering mechanism discussed in Sec. 4a.

It should be noted that for carrier scattering by the homopolar optical modes (20) the variational method gives a rate of entropy production which is proportional to k_x^2. According to (A12) the scattering sum then contains two terms and the temperature dependence of mobility has the form $(e^{\hbar\omega/kT}-1)[1+\frac{1}{2}(\hbar\omega/kT)]^{-1}$ given in Ref. (1) which agrees with the exact result derived in Sec. 4a only at high enough temperatures.

5. DISCUSSION

Comparing the experimental data on GaSe, MoS_2, $MoSe_2$, and WSe_2 with the theoretical results of the preceding section, we can now determine which scattering mechanism limits the carrier mobilities in these layer structures. To facilitate this comparison we have plotted in Fig. 9 the exponents n in

$$\mu=\mu_0(T/300°\text{K})^{-n}$$

for homopolar- (a), polar- (b), and acoustic- (c) mode scattering in accordance with Eqs. (26), (36), and (19) as functions of the energy $\hbar\omega$. From this figure it readily follows that acoustic-mode scattering cannot explain the experimental findings. Moreover, since $n_{\text{pol}}=n_{\text{hom}}-1$, it also follows that considerably higher phonon energies are required if the strong temperature dependence of μ is to be ascribed to polar rather than to homopolar scattering. As illustrated by the reststrahlen energies marked in Fig. 9, such high phonon energies are only met in compounds with light components, e.g. in oxides, and we therefore conclude that among the considered scattering mechanisms only the homopolar one is compatible with the experiment.

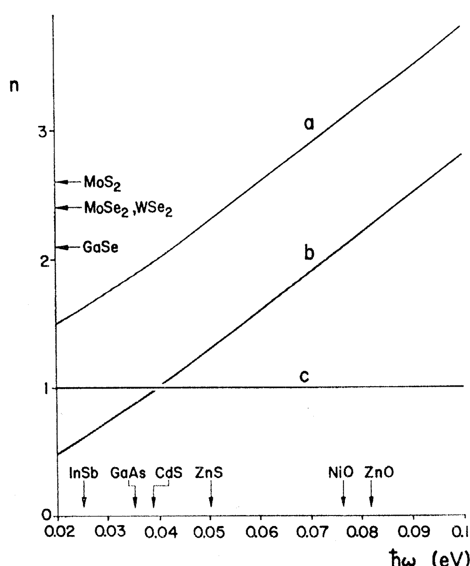

FIG. 9. The exponent n in $\mu=\mu_0(T/T_0)^{-n}$ for (a) interaction with homopolar optical modes, (b) interaction with polar optical modes, (c) interaction with acoustic modes.

The above conclusion rests on the strong temperature dependence of the carrier mobilities in layer structures. A word is therefore in order about the lead salt semiconductors in which n values as high as 2.5 have been observed for both electrons and holes.[19] Recently these large exponents have been attributed to scattering resulting from transitions between valence and conduction bands.[20,21] In the investigated layer structures we need not, however, consider this kind of scattering because all of them have large energy gaps ($1-2$ eV [9,22,23]) and band mixing therefore is negligible. Moreover, the temperature coefficient of the energy gap in the layer structures is negative whereas a positive one is needed to explain large n values on the basis of interband scattering.

The holes in diamondlike semiconductors also have highly temperature-dependent mobilities ($2<n<3$). The origin of this dependence is still uncertain: Nonparabolicity of the light hole band has been made at least partly responsible[24] although nonpolar optical scattering[25,26] is generally assumed to contribute largely to it. Since in GaSe electron and hole mobilities have the same n values, the nonparabolicities of valence and conduction band would have to be similar if they were to account for the observed temperature dependences.

[19] W. W. Scanlon, *Solid State Physics*, edited by F. Seitz and D. Turnbull (Academic Press Inc., New York, 1959), Vol. 8. p. 83.
[20] B. S. Krishnamurthy and K. P. Sinha, J. Phys. Chem. Solids **26**, 1949 (1965).
[21] Yu. I. Ravich, Fiz. Trevd. Tela **7**, 1821 (1965) [English transl.: Soviet Phys.—Solid State **7**, 1466 (1965)].
[22] R. F. Frindt, J. Phys. Chem. Solids **24**, 1107 (1963).
[23] R. F. Frindt and A. D. Yoffe, Proc. Roy. Soc. (London) **A273**, 69 (1963).
[24] R. Keiper and H. W. Streitwolf, Phys. Status Solidi **12**, K21 (1965).
[25] H. Ehrenreich and A. Overhauser, Phys. Rev. **104**, 331, 649 (1956).
[26] K. B. Tolpygo and H. M. Fedorchenko, Zh. Experim. i Teor. Fiz. **31**, 845 (1957) [English transl.: Soviet Phys.—JETP **4**, 713 (1957)].

In view of the band calculations[27,28] available at present, this would seem to be highly unlikely. The nonpolar optical scattering, on the other hand, which contributes to the temperature dependence of the hole mobility in diamondlike semiconductors is similar to the homopolar scattering considered here. However, because of the large difference between the strength of the interlayer bonding and that of the intralayer bonding, the relevant potential gradients are much larger in layer structures. Optical scattering is therefore expected to dominate instead of being merely comparable to acoustic scattering as e.g., in Ge.[29]

From Fig. 4 it follows that the electrons and holes in GaSe couple to the same lattice mode which according to Fig. 9 has an energy $\hbar\omega \approx 0.04$ eV. In order to compare this energy with recent data on infrared reflectivity[16] and Raman spectra[30,31] a simple analysis was made of the motion of the four atoms in the unit cell of a layer of GaSe. According to this analysis two homopolar modes exist in GaSe with polarization normal to the layers, i.e., a low frequency one in which the Ga and Se atoms vibrate in phase and a high frequency one in which they move in counterphase. It can be shown that if the stretching force constant of the Ga–Ga bond is smaller than or equal to that of the Ga–Se bond then the energy of the high-frequency mode is somewhat higher than that of the lattice mode responsible for the reststrahlen absorption of radiation propagating along the normal to the layers. For this mode Leung *et al.*[16] have found $\hbar\omega = 0.029$ eV, so that with its somewhat higher energy the homopolar high-frequency mode readily accounts for the measured n values. This identification of the phonon with which the carriers in GaSe interact gains further support from a discussion of the infrared and Raman activity of the different modes derived from the present analysis. On the basis of this discussion Brebner[32] has made a tentative assignment of all the Raman lines observed by Wright and Mooradian[31] which attributes an $\hbar\omega = 0.038$ eV to the relevant mode.

The Ga and Se atoms vibrate in counterphase in the high-frequency mode which therefore deforms the Ga–Se bonds more than the Ga–Ga bonds. Since our experiment shows that both kinds of charge carriers interact with this mode it follows that both of them must have their maximum density between the Ga and Se planes of each layer, and this is confirmed by the band calculations of Bassani and Pastori Parravicini.[28] As shown by these authors the edge of the conduction band occurs at the center Γ of the Brillouin zone. In the tight binding approximation the corresponding state Γ_3^+ is formed by linear combinations of the p_x and p_y orbitals of the Ga and Se atoms. It is symmetrical with respect to the mirror plane of the layer and does indeed lead to maximum charge density between the Ga and Se planes. Moreover, the valence band edge was reported to be formed by the state Γ_1^+. However, this identification of the valence band edge seems doubtful. Near the absorption edge of GaSe Brebner, Halpern, and Mooser[33] have in fact observed optical transitions between states of like symmetry as well as between states of unlike symmetry. This observation can be understood only if the nearly degenerate symmetric and antisymmetric states Γ_3^+ and Γ_3^- form the valence band edge and do not lie below it as was suggested in Ref. 27. Such a reidentification of the valence band edge is all the more justified because it involves only insignificant changes of the parameters on which the band calculations are based. Like Γ_3^+, the state Γ_3^- is made up of linear combinations of p_x and p_y functions of all Ga and Se atoms. Since the p_x and p_y functions of the atoms to one side of the mirror plane do not overlap very much with those of the atoms to the other side of this plane, the charge densities along the z axis corresponding to the states Γ_3^+ and Γ_3^- are essentially the same. Regardless of whether the holes giving rise to the p-type conduction have symmetrical or antisymmetrical wave functions, the deformation potential determining their scattering will therefore be very nearly the same as that determining the scattering of the electrons.

Because there are only three atoms in the unit cell of a MoS_2 layer there exists in the MoS_2 type of compounds only one vertically polarized homopolar mode. It corresponds to a counterphase movement of the chalcogene atoms along the z axis, the transition-metal atoms remaining at rest in the mirror plane of each layer. If therefore the electron and hole mobilities are limited by vertical-mode scattering then their temperature dependences should be the same. However, it should be noted that as long as the band structures of the MoS_2 phases are not known one cannot ascertain that the deformation potentials of electrons and holes are as closely similar as they are in GaSe. The vertical-mode scattering mechanism therefore need not apply to holes although experiment has established its relevance for the electrons. According to Fig. 9 the exponents $n = 2.6$, and $n = 2.4$ derived from the electron mobilities of MoS_2 and from those of $MoSe_2$ and WSe_2, respectively, lead to energies $\hbar\omega \approx 0.06$ eV and $\hbar\omega \approx 0.05$ eV for the relevant model. These energies agree well with expectation: Those corresponding to the selenides should differ only slightly from one another and both of them should be smaller than that cor-

[27] H. Kamimura and K. Nakao, in *Proceedings International Conference of the Physics of Semiconductors* [J. Phys. Soc. Japan, Suppl. **21**, 27 (1966)].
[28] F. Bassani and G. Pastori Parravicini, Nuovo Cimento **B50**, 95 (1967).
[29] W. A. Harrison, Phys. Rev. **104**, 1281 (1956).
[30] J. P. Russel (private communication).
[31] G. B. Wright and A. Mooradian, Bull. Am. Phys. Soc. **11**, 812 (1966).
[32] J. L. Brebner (private communication).
[33] J. L. Brebner, J. Halpern, and E. Mooser, Helv. Phys. Acta **40**, 382 (1967); J. L. Brebner, J. Phys. Chem. Solids **25**, 1427 (1964); Helv. Phys. Acta **37**, 589 (1964).

TABLE II. The experimental values of the parameters of the theory.

Compound	Cond. type	$\frac{m_x}{m}$	$\hbar\omega$ (eV)	$g^2\frac{m_x}{m}$	g^2	$\frac{\epsilon_z}{a}\frac{m_x}{m}$ (eV/Å)	$\frac{\epsilon_z}{a}$ (eV/Å)	$a(m/m_x)^{1/3}$ (Å)	a (Å)	$2d_{C-A}$ (Å)
GaSe	n	0.2	0.04	0.033	0.17	2.2	11.0	5.2	3.0	2.4
	p	0.44	0.04	0.17	0.38	5.0	11.0	3.9	3.0	
MoS_2	n		0.06	0.13		4.4		4.1		3.0
$MoSe_2$	n		0.05	0.1		5.5		3.8		3.2
WSe_2	n		0.05	0.1		5.5		3.8		3.2

responding to the sulfide. Unfortunately, we were unable to measure the intrinsic hole mobilities so that a comparison between the n values of electrons and holes is impossible at present.

In Table II we have listed the vibrational energies, the coupling constants g^2 and the ratios ϵ_z/a as derived from the measured mobilities according to Eqs. (26), (24), and (21). In these equations g^2 and ϵ_z/a appear weighted with the ratio m_x/m of the effective carrier mass m_x in the x,y plane and the electron mass m. In the case of GaSe this ratio is known for both electrons and holes. Thus, from magneto-optical measurements Halpern[34] and Sugano *et al.*[35] have found a reduced mass $(m_{xe}m_{xh}/m_{xe}+m_{xh})=0.14m$ for electrons and holes in the plane of the layers. Together with the ratio $m_{xe}/m_{xh} = (\mu_h/\mu_e)^{1/2}=1/\sqrt{5}$ derived from our mobility measurements one therefore has $m_{xe}/m=0.2$ and $m_{xh}/m=0.44$. The coupling constant for holes obtained from these values closely approaches the limit $g_{\mathrm{crit}}^2=\frac{1}{2}$ above which self-trapping occurs. Nevertheless, the corresponding deformation potentials are not unduly large. Thus we note that if measured per unit dilatation $\delta V/V$ the deformation potential relevant for the holes in covalent semiconductors normally are of the order of the first atomic ionization potential[36] I. With $\delta V/V=3\delta a/a$ the variation ϵ_z/a of energy per unit variation of the diameter a of the Wigner-Seitz cell is equal to $\epsilon_z/a = I$[eV/Å], where for convenience $a=3$ Å. Since the first ionization potentials of Ga and Se are 6 and 9 eV, respectively, the value $\epsilon_z/a=11$[eV/Å] is indeed reasonable. As a further confirmation of the compatibility of theory and experiment we have equated a to the widths of the square potential well in which a particle of mass m has the deformation potential $d\epsilon/da=\epsilon_z/a$, where $\epsilon=\nu^2\pi^2\hbar^2/2ma^2$. Since the carrier densities are highest between the cation and anion planes on either side of the center of a layer, we have in this equivalence taken $\nu=2$, so that the corresponding wave function has a node in the center of the well. Comparison with the last two columns of the table then shows that the widths of the wells are indeed close to twice the distance d_{C-A} between neighboring cation and anion layers.

6. CONCLUSIONS

Measurements of Hall effects and resistivity carried out on a series of semiconducting layer structures have shown that in these materials the charge carriers have rather low but strongly temperature-dependent mobilities. It follows from our discussion that these findings can best be interpreted in terms of a short-range interaction coupling the carriers to those optical modes of the lattice which modulate the layer thickness. The interaction is thus specific of layer structures and reflects the tendency in these structures of the charge carriers to become localized within individual layers. Where possible, comparison of theory and experiment leads to excellent agreement.

ACKNOWLEDGMENTS

The authors wish to express their thanks to Dr. J. L. Brebner for many helpful suggestions, to R. Béchade and P. Steiger for their help with the electric measurements, and last but not least to H. U. Boelsterli for the preparation of the single crystals.

APPENDIX: THE CALCULATION OF SCATTERING SUMS

The scattering sums in (8) and (32) are of the form

$$F(\mathbf{p})=\sum_{p',k}\phi(\mathbf{k})\delta[\epsilon_{p'}-(\epsilon_p\pm\hbar\omega)]\delta(\mathbf{p}',\mathbf{p}\pm\hbar\mathbf{k}), \quad \text{(A1)}$$

where $\phi(\mathbf{k})$ depends on the physical quantity considered and where the signs + and − refer to phonon absorption and emission, respectively. Since according to (11) the carrier energy depends very little on the z component of momentum, the following separation is possible:

$$F(\mathbf{p})=\sum_{p_x',k_x}\bar{\phi}(\mathbf{k}_x)\delta[\epsilon_{p_x'}-(\epsilon_{p_x}\pm\hbar\omega)] \times\delta(\mathbf{p}_x',\mathbf{p}_x\pm\hbar\mathbf{k}_x), \quad \text{(A2)}$$

where

$$\bar{\phi}(\mathbf{k}_x)=\sum_{p_z',k_z}\phi(\mathbf{k})\delta(\mathbf{p}_z',\mathbf{p}_z\pm\hbar\mathbf{k}_z)=\sum_{k_z}\phi(\mathbf{k}) \quad \text{(A3)}$$

is averaged over $\mathbf{k}_z$ and depends only on $\mathbf{k}_x$. The summa-

[34] J. Halpern, in *Proceedings of the International Conference of the Physics of Semiconductors* [J. Phys. Soc. Japan, Suppl. **21**, 180 (1966)].

[35] K. Aoyagi, A. Misu, G. Kuwabara, Y. Nishina, S. Kurita, T. Fukuroi, O. Akimoto, H. Hasegawa, M. Shinada, and S. Sugano, in *Proceedings of the International Conference of the Physics of Semiconductors* [J. Phys. Soc. Japan, Suppl. **21**, 174 (1966)].

[36] W. Ehrenberg, *Electric Conduction in Semiconductors and Metals* (Clarendon Press, Oxford, England, 1958), Chap. 7.

tions are then carried out in the usual manner: First the δ function of momentum is replaced by the constraint

$$p_x'^2=p_x^2+\hbar^2k_x^2\pm 2p_x\hbar k_x\cos\theta\,, \qquad (A4)$$

where θ is the angle between $\mathbf{p}_x$ and $\mathbf{k}_x$. Next the sums are written in the form

$$F(\mathbf{p})=\int\phi(\mathbf{k})\delta\left[\epsilon\left(\alpha^2\pm 2\alpha\cos\theta\pm\frac{\hbar\omega}{\epsilon}\right)\right]\frac{2m\epsilon}{\hbar^2}\times\alpha d\alpha d\theta dk_z/8\pi^3\,, \qquad (A5)$$

in which the following abbreviations have been introduced:

$$\epsilon=p_x^2/2m_x\,,\quad \alpha=\hbar k_x/p_x\,,\quad d\mathbf{k}_x=d\theta(p_x/\hbar)^2\alpha d\alpha. \qquad (A6)$$

Unlike the three-dimensional case, the δ function of energy cannot be eliminated by integration over $\cos\theta$. Instead we have to integrate over α making use of the property

$$\int f(\alpha)\delta[g(\alpha)]d\alpha=\sum_n\frac{f(\alpha_n)}{|(dg/d\alpha)(\alpha_n)|} \qquad (A7)$$

of the δ functions, where $f(\alpha)$ and $g(\alpha)$ are continuous functions of α and where the α_n are the n roots of $g(\alpha)=0$.

We distinguish between phonon absorption and phonon emission. In the first case $g(\alpha)$ has a single positive root

$$\alpha^+=-\cos\theta+(\cos^2\theta+\hbar\omega/\epsilon)^{1/2}\,,$$

all angles $0\leqq\theta\leqq 2\pi$ are allowed, and one finds

$$F^+(\mathbf{p})=\int_0^{2\pi}\frac{m_x}{\hbar^2}\frac{\alpha^+\phi(p_x\alpha^+/\hbar,k_z)}{(\cos^2\theta+\hbar\omega/\epsilon)^{1/2}}d\theta dk_z/8\pi^3. \qquad (A8)$$

In the second case $g(\alpha)$ has the two positive roots

$$\alpha_{1,2}^-=\cos\theta\pm(\cos^2\theta-\hbar\omega/\epsilon)^{1/2}\,,$$

and only angles $\theta\leqq\theta_0=\cos^{-1}(\hbar\omega/\epsilon)^{1/2}$ are admissible. Moreover, for $\epsilon<\hbar\omega$ the integral is zero and one has

$$F^-(\mathbf{p})=\int_{-\theta_0}^{\theta_0}\frac{m_x}{\hbar^2}\times\frac{\alpha_1^-\phi(p_x\alpha_1^-/\hbar,k_z)+\alpha_2^-\phi(p_x\alpha_2^-/\hbar,k_z)}{(\cos^2\theta-\cos^2\theta_0)^{1/2}}d\theta dk_z/8\pi^3 \qquad (A9)$$

for $\epsilon\geqq\hbar\omega$.

In connection with the calculation of mobility three different $\phi(\mathbf{k})$ must be considered:

(a) $\phi(\mathbf{k})=A=\text{const}$. From (A8) one finds

$$F^+(\mathbf{p})=\frac{m_x}{\hbar^2}A\,2\pi\frac{N_z}{4\pi^2}=\frac{m_xN_z}{2\pi\hbar^2}=D_2A\,, \qquad (A10)$$

where D_2 is the two-dimensional density of states (12). Furthermore, with the substitutions $y=\sin\theta$ and $y_1=(1-\hbar\omega/\epsilon)^{1/2}$ (A9) leads to

$$F^-(\mathbf{p})=\frac{m_x}{\hbar^2}A\frac{N_z}{4\pi^2}\int_{-y_1}^{y_1}\frac{2dy}{y_1^2-y^2}=\frac{m_xN_z}{2\pi\hbar^2}A=D_2A=F^+(\mathbf{p})\,. \qquad (A11)$$

(A10) and (A11) are of course trivial since with $\phi(\mathbf{k})=1$ (A1) is the very definition of the density of states at the energies $\epsilon_p\pm\hbar\omega$.

(b) $\phi(\mathbf{k})=Bk_x^2$. Since odd powders of $\cos\theta$ do not contribute in this case one has

$$F^+(\mathbf{p})=2\frac{m_x^2}{\hbar^2}\epsilon\frac{N_zB}{4\pi^2}\int_0^{2\pi}\left(3\cos\theta+\cos^2\theta+\frac{\hbar\omega}{\epsilon}\right)d\theta=\frac{m_x}{\hbar^2}BD_2\left(\epsilon+\frac{\hbar\omega}{2}\right). \qquad (A12)$$

(c) $\phi(\mathbf{k})=C(k_x^2/k^2)=C(k_x^2/k_x^2+k_z^2)$. The average $\bar\phi(\mathbf{k})$ over $\mathbf{k}_z$ then is

$$\bar\phi(\mathbf{k}_x)=\sum_{k_z}\frac{C}{1+k_z^2/k_x^2}=C\int_{-\pi/d_z}^{\pi/d_z}\frac{dk_z/2}{1+k_z^2/k_x^2}=Ck_x\frac{\tan^{-1}(\pi/k_xd_z)}{\pi} \qquad (A13)$$

which for $\mathbf{k}_x=0$ is equal to $C(\frac{1}{2}k_x)$. $\bar\phi(k_x)$ is significantly lower than this only for $k_x\simeq\pi/d_z$, i.e. for absorption processes involving carriers which are at least 0.5 eV away from the band edge. Since their number is very small $\bar\phi(k_x)$ can be approximated by its value $\bar\phi(0)$ over the whole energy range and one has

$$F^+(\mathbf{p})=\bar\phi(0)\int_0^{\pi/2}\frac{4m_x}{\hbar^2}\frac{p_x}{\hbar}\frac{2\cos^2\theta+\hbar\omega/\epsilon}{(\cos^2\theta+\hbar\omega/\epsilon)^{1/2}}\frac{d\theta}{4\pi^2}$$

which to within an accuracy of about 20% is equal to

$$F^+(\mathbf{p})\cong\frac{C}{4\pi}\left(\frac{m}{\hbar^2}\right)^{3/2}[(\hbar\omega)^{1/2}+\epsilon^{1/2}]. \qquad (A14)$$